

Reverse and Multiple Stable Isotope Probing to Study Bacterial Metabolism and Interactions at the Single Cell Level

Yun Wang,[†] Yizhi Song,[‡] Yifan Tao,[§] Howbeer Muhamadali,^{||} Royston Goodacre,^{||} Ning-Yi Zhou,[⊥] Gail M. Preston,[#] Jian Xu,^{*,†} and Wei E. Huang^{*,‡}

[†]Single Cell Center, CAS Key Laboratory of Biofuels and Shandong Key Laboratory of Energy Genetics, Chinese Academy of Sciences, Qingdao, 266101, P. R. China

[‡]Department of Engineering Science, University of Oxford, Parks Road, Oxford, OX1 3PJ, United Kingdom

[§]Department of Operative Dentistry and Endodontics, Guanghua School and Hospital of Stomatology, Sun Yat-sen University, Guangzhou, 510055, P. R. China

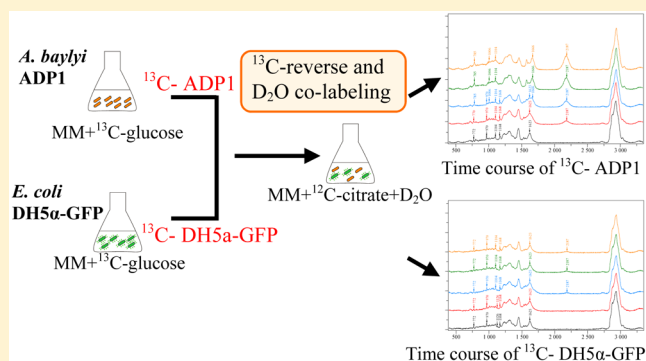
^{||}School of Chemistry, Manchester Institute of Biotechnology, University of Manchester, 131 Princess Street, Manchester, M1 7DN, United Kingdom

[⊥]State Key Laboratory of Microbial Metabolism and School of Life Sciences & Biotechnology, Shanghai Jiao Tong University, Shanghai, 200240, P. R. China

[#]Department of Plant Sciences, University of Oxford, South Parks Road, Oxford OX1 3RB, United Kingdom

S Supporting Information

ABSTRACT: The interactions between microorganisms driven by substrate metabolism and energy flow are important to shape diversity, abundance, and structure of a microbial community. Single cell technologies are useful tools for dissecting the functions of individual members and their interactions in microbial communities. Here, we developed a novel Raman stable isotope probing (Raman-SIP), which uses Raman microspectroscopy coupled with reverse and D₂O co-labeling to study metabolic interactions in a two-species community consisting of *Acinetobacter baylyi* ADP1 and *Escherichia coli* DH5α-GFP. This Raman-SIP approach is able to detect carbon assimilation and general metabolic activity simultaneously. Taking advantage of Raman shift of single cell Raman spectra (SCRS) mediated by incorporation of stable-isotopic substrates, Raman-SIP with reverse labeling has been applied to detect initially ¹³C-labeled bands of ADP1 SCRS reverting back to ¹²C positions in the presence of ¹²C citrate. Raman-SIP with D₂O labeling has been employed to probe metabolic activity of single cells without the need of cell replication. Our results show that *E. coli* alone in minimal medium with citrate as the sole carbon source had no metabolic activity, but became metabolically active in the presence of ADP1. Mass spectrometry-based metabolite footprint analysis suggests that putrescine and phenylalanine excreted by ADP1 cells may support the metabolic activity of *E. coli*. This study demonstrates that Raman-SIP with reverse labeling would be a useful tool to probe metabolism of any carbon substrate, overcoming limitations when stable isotopic substrates are not readily available. It is also found that Raman-SIP with D₂O labeling is a sensitive and reliable approach to distinguish metabolically active cells but not quiescent cells. This novel approach extends the application of Raman-SIP and demonstrates its potential application as a valuable strategic approach for probing cellular metabolism, metabolic activity, and interactions in microbial communities at the single cell level.



Microorganisms play fundamental roles during natural biogeochemical cycles of the biosphere and human biological processes, and thus studying their functions and activity *in situ* is of great importance.¹ In the natural environment, microorganisms usually exist in complex communities, so substrate metabolism and energy flow in these communities are inevitably intertwined by competition and cooperation among community members.² Although biological, physical, and chemical interactions have significant impact on structure, diversity, and stability of a microbial

community, the metabolic interactions of cells in these communities are important drivers to microbial interactions.³

Metagenomics provide an overall picture of microbial diversity, abundance, structure, and the potential functional genes present in a natural community.^{4,5} The next questions are what the active functions of individual members in a

Received: April 23, 2016

Accepted: September 2, 2016

Published: September 2, 2016

community are and how they interact.² The majority (over 99%) of microorganisms in the natural environment are not yet cultivated under laboratory conditions,⁶ and cell phenotypes and behaviors are usually different in a pure culture compared to their biological context in microbial communities. Moreover, functional validation cannot be achieved without an effective strategy for identification of cellular phenotypes.⁷ These challenges emphasize the importance of single cell study of microbial metabolism and their interactions within communities.^{8,9}

The application of single cell technologies may provide further insights into microbial communities, allowing linkage of specific metabolic activities to the relevant community members. To date, single cell technologies have been applied to diverse ecological niches including marine,¹⁰ freshwater,¹¹ soil¹² and human subgingival crevice,¹³ etc. Among these single cell techniques, Raman microspectroscopy is a label-free and nondestructive tool, compared to fluorescence-based approaches and mass spectrometry (MS), enabling the biochemical investigation of microbes in their natural habitat.¹⁴ A single cell Raman spectrum (SCRS) is defined as the “biochemical fingerprint” of a cell, which reflects comprehensive intrinsic biochemical information. Combination of Raman microspectroscopy with stable isotope labeling (Raman-SIP) has been demonstrated to be a promising approach for understanding the complex metabolic behavior of various microbial communities, as some Raman bands of SCRS shift to lower wavenumbers when ¹³C and ¹⁵N from substrates are incorporated into cells.^{15–18} Raman-SIP has been applied to probe substrate-specific metabolic pathways^{17–19} and carbon flow in a food chain.²⁰ One problem is that many isotope substrates are either unavailable (for example, there is no ¹³C fully labeled citrate) or very expensive. Initial labeling of cells using readily available ¹³C substrates (e.g., ¹³C-glucose) and then detecting reverse shift of SCRS may overcome the problem. Another problem is that ¹³C-Raman-SIP alone may not be adequate to study metabolism, as metabolic activity can be independent of carbon substrate incorporation. This leads to the insensitivity of ¹³C-Raman-SIP to detect cellular metabolic activity for substrate turnover when there is insufficient carbon incorporation. However, the application of heavy water (D₂O) to probe microbial community may be sensitive enough to unravel general metabolic activity without cell reproduction.²¹

In this study, we applied Raman-SIP with ¹³C-reverse and D₂O co-labeling to monitor substrate metabolism, cell activity, and their interactions of a two-species community consisting of *Acinetobacter baylyi* ADP1 and *Escherichia coli* DH5 α -GFP. While Raman-SIP with ¹³C-reverse labeling revealed the carbon flow, D₂O labeling was used to unravel the energy flow and general metabolic activity. In this reverse labeling process, ¹²C-substrates (citrate in this study) were introduced into a co-culture in which all cells were initially ¹³C-labeled. ¹³C-cells that can metabolize the ¹²C-substrate were reverted to ¹²C-cells in a time-dependent manner, which were quantified by Raman reverse-shift in SCRS. *E. coli* alone in minimal medium with citrate as the sole carbon source had no metabolic activity, but became metabolically active in the presence of ADP1. Metabolite footprint analysis using gas chromatography/mass spectrometry (GC/MS) confirms the Raman-SIP results.

■ EXPERIMENTAL METHODS

Strains and Growth Conditions. All chemicals in this study were obtained from Sigma-Aldrich U.K.

Escherichia coli DH5 α -GFP used in this study contained a modified p18GFP plasmid²² which constitutively expresses a *gfp* gene. *Acinetobacter baylyi* ADP1 and DH5 α -GFP were cultured in minimal medium (MM)²³ supplemented with appropriate carbon sources at 37 °C, with 150 rpm shaking. When required, 100 μ g/mL ampicillin was added into the medium to cultivate DH5 α -GFP and ADP1 separately or together. Wild type ADP1 can grow in a medium with 100 μ g/mL ampicillin because it contains a gene encoding AmpC β -lactamase in the chromosome.²⁴ MM with 5 g/L glucose (MMG) of ¹²C-D-glucose/99% uniformly labeled ¹³C-D-glucose or 10 mM citrate (MMC) were used to cultivate cells. MMC with a final concentration of 40% “heavy water” (D₂O, 99.9 atom % D, Sigma-Aldrich, Germany) was used for the deuterium labeling experiment.

To examine cell growth, ADP1 and DH5 α -GFP were initially incubated in LB with ampicillin (100 μ g/mL) overnight. Cells were then harvested by centrifugation at 3000 g and washed twice with minimal medium and resuspended in the same volume of MM. Then 250 μ L of the cell suspension were inoculated into 5 mL of MM or MMC. Aliquots (200 μ L) of the inoculated media were transferred into a 96-well plate and the growth profiles were recorded by measuring the optical density at 600 nm every 15 min using a microplate reader (Synergy HT, BioTek). Five biological replicates were carried out for each condition.

A schematic of co-culture experiment using reverse and D₂O labeling is shown in Figure S1. Generally, ¹²C-, ¹³C-cells of ADP1, DH5 α -GFP or mixture of ADP1–DH5 α -GFP grown in ¹²C- or ¹³C-MMG overnight were washed, 1:10 diluted by MM and introduced into 20 mL of MMC with 100 μ g/mL of ampicillin with or without 40% D₂O in the form of either pure culture or co-culture. Cell counting was performed using a hemocytometer under a fluorescent Raman microscope.²⁵ In the co-culture, DH5 α -GFP cells contain constitutively expressed green fluorescent protein (GFP), thus can be readily distinguished from ADP1 under a Raman-fluorescent microscope.¹⁷ The initial cell densities of ADP1 and DH5 α -GFP were $\sim 0.7 \times 10^8$ and 1.1×10^8 CFU/mL separately. Co-culture cells were incubated on a shaker at 37 °C, 120 rpm and sampled at 0, 1, 2, 4, and 7 h for Raman measurement. The supernatants were collected and stored at –80 °C for metabolic footprint analysis, described in detail below. Three biological replicates were carried out for each condition.

Raman Microspectroscopy Analysis. All of the cell samples were washed with dionized water three times to remove the culture medium. Cell density was adjusted accordingly to ensure sufficient dispersion of individual cells on the slide. After washing and resuspending, a 1.5 μ L cell suspension was transferred onto a calcium fluoride (CaF₂) slide and air-dried prior to Raman analysis. Raman spectra were obtained using a modified confocal Raman-fluorescent microscope based on LabRam HR (Horiba Ltd., U.K.) as previously described.²⁵ A 100 \times magnifying dry objective (NA = 0.90, Olympus, U.K.) was used for sample observation and Raman signal acquisition. A 532 nm Nd:YAG laser (Ventus, Laser Quantum Ltd., U.K.) was used as the light source for Raman measurement, and the power on the sample was 3–5 mW. The acquisition time for each spectrum was 10 s. The scattered photons were collected by a Newton EMCCD (DU970N-BV, Andor, U.K.). A 300 grooves/mm diffraction grating was used for most of the measurements unless otherwise stated, resulting

in a spectral resolution of $\sim 2 \text{ cm}^{-1}$ with 1581 data points spanning the range 394–3341 cm^{-1} .

Data Analysis of Raman Spectra. The Raman spectra were processed by background subtraction (using spectra of the cell free regions on the same slide), baseline correction, and normalization using the Labspec5 software (HORIBA Jobin Yvon Ltd., U.K.) before further analysis. For quantification of the degree of D substitution in C–H bonds (% C–D), the bands assigned to C–D (2040–2300 cm^{-1}) and C–H (2800–3100 cm^{-1}) were calculated using integration of the specified region.²¹ Since the presence of D₂O made the $\sim 1006 \text{ cm}^{-1}$ band (C–C aromatic ring stretching of phenylalanine²⁶) split into two sharp bands (~ 1006 and 994 cm^{-1}), integrations of the region 1001–1009 cm^{-1} and 987–995 cm^{-1} were combined together to indicate ^{12}C replacement, while integration of the region 963–971 cm^{-1} was used to represent ^{13}C incorporation.

Metabolic Footprint Analysis. Samples were taken from each of the growth conditions as 500 μL aliquots and centrifuged at 4 $^{\circ}\text{C}$, 5000 g for 10 min using a microcentrifuge (5415R, Eppendorf). The supernatants were transferred into new microcentrifuge tubes, flash frozen in liquid nitrogen for 1 min, and stored at $-80 \text{ }^{\circ}\text{C}$ until further analysis. Cell pellets were discarded. Upon analysis, 50 μL aliquots from each of the samples were combined in a new 15 mL Falcon tube to be used as quality control (QC) samples.²⁷ Internal standard solution (0.2 mg mL^{-1} succinic- d_4 acid, 0.2 mg mL^{-1} glycine- d_5 , 0.2 mg mL^{-1} benzoic- d_5 acid, and 0.2 mg mL^{-1} lysine- d_4) was added as a 100 μL aliquot to all the samples (including QCs), followed by an overnight drying step using a speed vacuum concentrator (Concentrator 5301, Eppendorf, Cambridge, U.K.). The dried pellets were derivatized following a two-step procedure, which include oximation (using methoxyamine-hydrochloride in pyridine) followed by a silylation step (using *N*-methyl-*N*-(trimethylsilyl) trifluoroacetamide).²⁸

All derivatized samples were analyzed using a Gerstel MPS-2 autosampler (Gerstel, Baltimore, MD), on an Agilent 6890N GC oven (Wokingham, U.K.) coupled to a Leco Pegasus III mass spectrometer (St. Joseph, MI) following previously published methods.^{29,30} Leco ChromaTOF software was employed to deconvolute the data, and subsequent identification of the peaks was carried out using an in-house library (Table S1) and following metabolomics standard initiative (MSI) guidelines.³¹

RESULTS

Reverse Labeling for Pure Cultures of *A. baylyi* ADP1 and *E. coli* DH5 α -GFP. SCRS of ^{12}C -labeled ADP1 and DH5 α -GFP bacteria showed ^{12}C characteristic Raman bands at 785 cm^{-1} (ring breathing modes in the DNA/RNA bases), 1006 cm^{-1} (ring breathing mode of benzene ring compounds; most notably from phenylalanine), 1666 cm^{-1} (protein band vibrations), and 2938 cm^{-1} (C–H vibration) (Figure S2A,B and Table 1). Correspondingly, SCRS of ^{13}C -labeled ADP1 and DH5 α -GFP had ^{13}C -shifted Raman bands at 772, 970, 1623, and 2930 cm^{-1} , indicating complete ^{13}C -substitution in cells (Figure 1A,B and Table 1). Figure S3 shows SCRS of *A. baylyi* ADP1 and *E. coli* DH5 α -GFP without labeling and with only ^2H or ^{13}C labeling as well as both labeling. Cells of ^{13}C -fully labeled *A. baylyi* ADP1 and *E. coli* DH5 α -GFP were separately prepared by growth in MM with ^{13}C -D-glucose as the sole carbon source. Cells were grown 16 h overnight to ensure full

Table 1. Representative Raman Band Shifts and Their Putative Assignments due to ^{13}C and ^2H Substitutions

wavenumber to ^{12}C -cells (cm^{-1})	wavenumber to ^{13}C -cells (cm^{-1})	wavenumber to ^2H cells (cm^{-1})	assignment	ref
785	770		cytosine, uracil (ring, str)	17
1006	970	994	ring breathing mode of benzene ring compounds	17,21
1126		1104	lipids	17,21
1168		1104	lipids	17,21
1666	1623		C=C stretching band	17
2938	2930	2040–2300 ^a	C–H vibration	17

^aPeak at 2187 cm^{-1} .

incorporation of ^{13}C into the cells. Then these ^{13}C -labeled ADP1 and DH5 α -GFP bacteria were transferred into fresh MMC to examine (so-called) reverse labeling. After 7 h of incubation, those initial ^{13}C -characteristic Raman bands of SCRS in ADP1 were reverted back to ^{12}C -positions at 785, 1006, 1666, and 2938 cm^{-1} (Figure 1A and Table 1), indicating that ^{13}C in ADP1 cells has been replaced by ^{12}C from citrate, which was the sole carbon source. When 40% D₂O is added, apart from the above ^{13}C -reverse bands, ADP1 cells also displayed additional bands at 994 and 2187 cm^{-1} which are the results of the incorporation of D into benzene ring and C–D formation (Figure 1A and Table 1). Since *A. baylyi* ADP1 is able to grow by using citrate as a sole carbon source while *E. coli* DH5 α -GFP cannot use citrate under aerobic condition^{32,33} (Figure S4), the SCRS of DH5 α -GFP did not show any changes after 7 h of incubation in MMC (Figure 1B), which confirms the inability of DH5 α -GFP to assimilate citrate. The results of reverse labeling and D₂O-combined labeling are consistent (Figure 1), suggesting that this strategy could link Raman spectra to carbon assimilation and general metabolic activity at the single cell level.

SCRS Dynamics of Reverse Labeling in the Co-culture of *A. baylyi* ADP1 and *E. coli* DH5 α -GFP. SCRS of ADP1 and DH5 α -GFP in their mixed co-culture with or without 40% D₂O were sampled and measured separately. In the co-culture, cells of *E. coli* DH5 α -GFP were distinguishable from *A. baylyi* ADP1 cells as they showed fluorescence (Figure S5).

Time-course SCRS of ^{12}C -labeled *A. baylyi* ADP1 and ^{12}C -*E. coli* DH5 α -GFP, which were coinoculated in MMC as a control, did not show any observable change of their SCRS throughout the whole time course (Figure 2A and Figure 3A). By contrast, cells in the co-culture starting from ^{13}C -labeled ADP1 and ^{13}C -labeled DH5 α -GFP bacteria in MMC performed differently. In 7 h of incubation, ^{13}C in the ADP1 cells was gradually replaced by ^{12}C , causing reverse shifts from ^{13}C Raman bands at 772, 970, 1623, and 2930 cm^{-1} back to ^{12}C Raman bands at 785, 1006, 1666, and 2938 cm^{-1} (Figure 2B and Table 1). The SCRS reverse shift of ^{13}C -labeled DH5 α -GFP was inconclusive (Figure 3B), suggesting the weak ^{12}C substitution in ^{13}C -DH5 α -GFP cells if there are any. These findings are consistent with the cell counting results of ADP1 and DH5 α -GFP in the co-culture, which indicate that while ADP1 cells were multiplying, DH5 α -GFP cells had no observable growth during the 7 h of cocultivation (Figure S6).

Interestingly, the SCRS under the co-culture condition with D₂O (40%) suggest that both ADP1 and DH5 α -GFP were

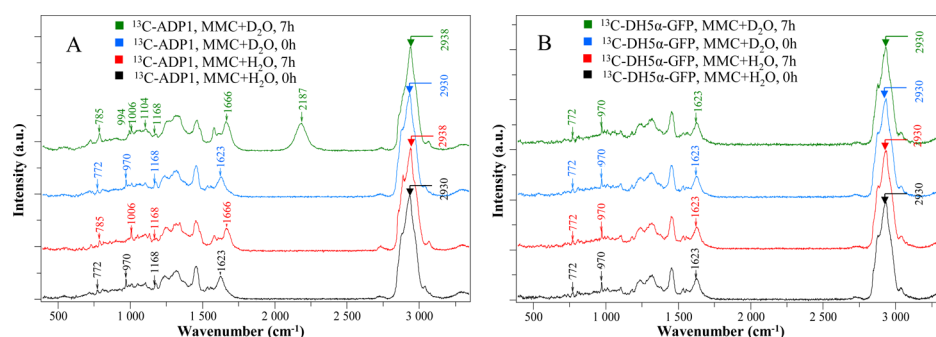


Figure 1. (A) Reverse labeling of *A. baylyi* ADP1 pure culture. SCRS of ^{13}C -labeled ADP1 cells grown in MMC with/without 40% D_2O . After 7 h of incubation, some bands of ^{13}C -SCRS shifted from 772, 970, 1623, and 2930 cm^{-1} back to ^{12}C -SCRS positions at 785, 1005, 1666, and 2938 cm^{-1} due to ^{12}C substitution of ^{13}C in cells, and the C–D band appeared around 2187 cm^{-1} in the presence of 40% D_2O . (B) Reverse labeling of *E. coli* DH5 α -GFP pure culture. SCRS of ^{13}C -labeled DH5 α -GFP cells grown in MMC with/without 40% D_2O . After 7 h of incubation, there was no observable change of 772, 970, 1623, or 2930 cm^{-1} , and no C–D band appeared around 2187 cm^{-1} in the presence of D_2O .

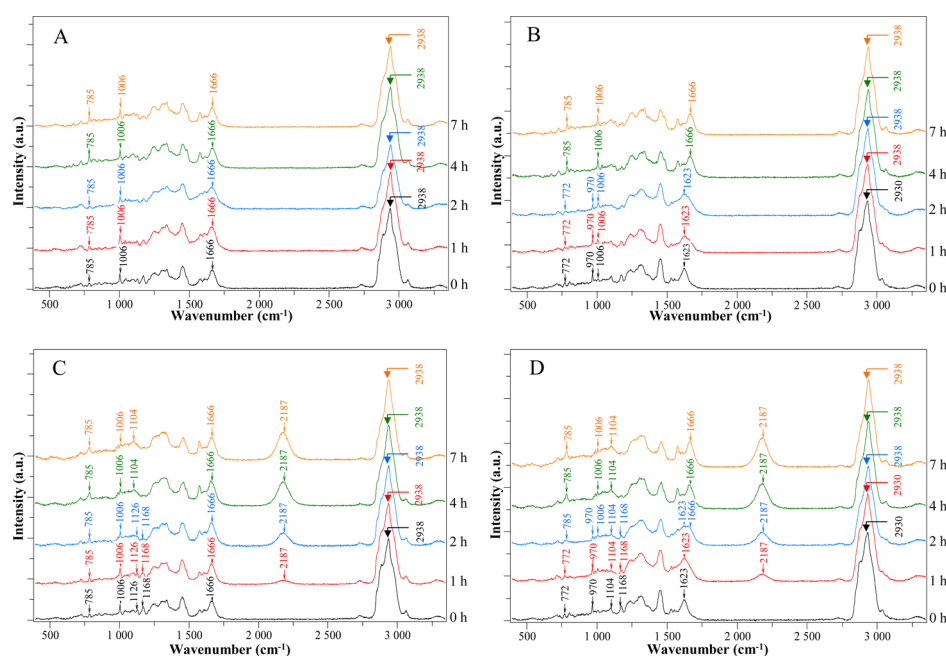


Figure 2. (A) Time-course of *A. baylyi* ADP1 SCRS from the co-culture of *A. baylyi* ADP1–*E. coli* DH5 α -GFP grown in MMC in H_2O as a control. During 7 h of incubation, there was no observable change of ^{12}C -SCRS positions. (B) Time-course of ^{13}C -labeled *A. baylyi* ADP1 SCRS from the co-culture of *A. baylyi* ADP1–*E. coli* DH5 α -GFP grown in MMC in H_2O . During 7 h of incubation, some bands of ^{13}C -SCRS gradually shifted from 772, 970, 1623, and 2930 cm^{-1} back to ^{12}C -SCRS positions at 785, 1005, 1666, and 2938 cm^{-1} . (C) Time-course of *A. baylyi* ADP1 SCRS from the co-culture of *A. baylyi* ADP1–*E. coli* DH5 α -GFP grown in MMC with 40% D_2O . During 7 h of incubation, there was no observable change of 785, 1006, 1666, or 2938 cm^{-1} . Because of deuterium incorporation, the C–D band appeared at 2187 cm^{-1} in 1 h and gradually increased its intensity, and lipid bands at 1168 and 1124 cm^{-1} shifted to 1104 cm^{-1} . (D) Time-course of ^{13}C -labeled *A. baylyi* ADP1 SCRS from the co-culture of *A. baylyi* ADP1–*E. coli* DH5 α grown in MMC with 40% D_2O . During 7 h of incubation, some bands of ^{13}C -SCRS gradually shifted from 772, 970, 1623, and 2930 cm^{-1} back to ^{12}C -SCRS positions at 785, 1005, 1666, and 2938 cm^{-1} . The C–D band appeared around 2187 cm^{-1} in 1 h and gradually increased its intensity, and the lipid band at 1168 cm^{-1} shifted to 1104 cm^{-1} .

metabolically active in the co-culture. SCRS showed that the C–D band around 2187 cm^{-1} was present after just 1 h for ADP1 (Figure 2C) and after 4 h for DH5 α -GFP (Figure 3C). The C–D band around 2187 cm^{-1} has been used previously as an indicator of general metabolic activity in cells.²¹ In addition, lipid bands at 1168 and 1124 also shifted to 1104 cm^{-1} due to deuterium incorporation (Figure 2C, 3C, and Table 1). Although *E. coli* DH5 α -GFP in MMC can neither grow nor show any metabolic activity (Figure S3 and Figure 1B), DH5 α -GFP in the presence of ADP1 in the co-culture displayed clear metabolic activity (Figure 3C). The delay of its general metabolic activity after 4 h suggests that DH5 α -GFP may

consume the metabolic byproducts of ADP1 which are excreted in the co-culture medium.

Double probing (reverse ^{13}C -labeling and D_2O probing) was also applied to the co-culture starting from ^{13}C -ADP1 and ^{13}C -DH5 α -GFP with 40% D_2O in MMC. These results show that in the initial ^{13}C characteristic bands in SCRS of ADP1 shifted back to ^{12}C positions, and the C–D band at 2187 cm^{-1} appeared after 1 h of incubation (Figure 2D). It was also observed that DH5 α -GFP became active after 2 h in the presence of ADP1 (Figure 3D). The results of D_2O and double labeling suggest that ADP1 metabolites were used by DH5 α -GFP to keep cells active but the metabolites were insufficient to

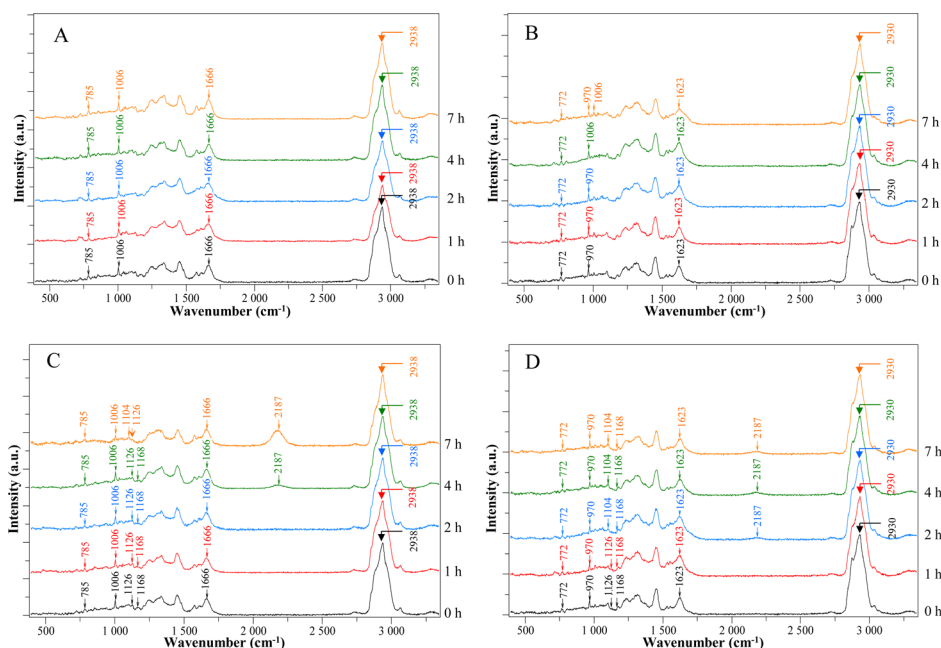


Figure 3. (A) Time-course of *E. coli* DH5 α -GFP SCRS from the co-culture of *A. baylyi* ADP1–*E. coli* DH5 α -GFP grown in MMC in H₂O as a control. During 7 h incubation, there was no observable change of ¹²C-SCRS positions. (B) Time-course of ¹³C-labeled *E. coli* DH5 α -GFP SCRS from the co-culture of *A. baylyi* ADP1–*E. coli* DH5 α -GFP grown in MMC in H₂O. During 7 h of incubation, the ¹³C-phenylalanine band slightly moved from 970 back to ¹²C-phenylalanine band position at 1006 cm^{−1}, but 772, 1623, and 2930 cm^{−1} did not shift. (C) Time-course of *E. coli* DH5 α -GFP SCRS from the co-culture of *A. baylyi* ADP1–*E. coli* DH5 α -GFP grown in MMC with 40% D₂O. During 7 h of incubation, the C–D band appeared at 2180 cm^{−1} in 4 h and gradually increased its intensity. (D) Time course of ¹³C-labeled *E. coli* DH5 α -GFP SCRS from the co-culture of *A. baylyi* ADP1–*E. coli* DH5 α grown in MMC with 40% D₂O. During 7 h of incubation, the ¹³C-SCRS positions did not shift obviously, and the C–D band appeared at 2187 cm^{−1} in 2 h.

support cell reproduction. This is also consistent to the cell counting results (Figure S6).

Dynamics of SCRS Characteristic Bands in the Co-culture. To measure the reverse shifts and C–D labeling quantitatively and to assess phenotypic heterogeneity of single cells, dynamic ratios of SCRS characteristic bands from ADP1 and DH5 α -GFP in the co-culture are plotted in Figure 4. Each point represents the average SCRS of 30 individual cells with three biological replicates. The relative intensity ratio of 970 to 1006 cm^{−1} was used to evaluate the ¹³C- reverse shift, and the relative intensity ratio of band CD peaked at 2187 cm^{−1} to CH + CD (2938 cm^{−1} + 2187 cm^{−1}) to assess general metabolic activity of cells. Integration of a region around the above-mentioned wavenumbers was used for calculation (more details are provided in the Experimental Methods). It shows that ¹³C-labeled vibrations at 970 cm^{−1} in ADP1 completely shifted back to ¹²C at 1006 cm^{−1} after 4 h of incubation (Figure 4A) and that DH5 α -GFP only partially reversely shifted back (Figure 4B). The increase of the CD/(CH + CD) ratio in ADP1 can be observed within 1 h and kept increasing in 7 h of incubation, indicating strong metabolic activity (Figure 4C). The ratio of CD/(CH + CD) in DH5 α -GFP also had a clear increase after 4 h, suggesting that DH5 α -GFP remained inactive at the beginning, and then became metabolically active with ADP1 when usable energy sources were present in the co-culture (Figure 4D).

Metabolic Footprint Analysis Confirmed That DH5 α -GFP Used Metabolites from ADP1 in the Co-culture. Although DH5 α -GFP alone cannot use citrate as the carbon source and it remained inactive in the MMC medium, the D₂O labeling results indicate that this *E. coli* strain had become metabolically active in the presence of ADP1 (Figure 3C,D and

Figure 4D). Among the 16 metabolites detected by GC/MS analysis of the footprint samples, putrescine and phenylalanine were abundant in the ADP1 pure culture, while these two metabolites were significantly reduced under the co-culture conditions. It is also worth noting that putrescine was absent in the DH5 α -GFP pure culture after incubating in MMC for 7 h (Figure 5). Prieto-Santos and colleagues³⁴ reported the ability of *E. coli* cells to utilize putrescine as the sole nitrogen, carbon, and energy source to support growth. These authors suggested that *E. coli* may catabolize putrescine to γ -amino-butylate, using putrescine- α -ketoglutarate transaminase and γ -aminobutyraldehyde dehydrogenase enzymes. Therefore, since *E. coli* is able to catabolize putrescine and phenylalanine,^{35,36} it is likely that putrescine and phenylalanine produced from ADP1 in the MMC co-culture supported metabolic activity of DH5 α -GFP (Figure 5).

DISCUSSION

Reverse Labeling Overcomes the Limits of Availability of ¹³C-Substrates. It has been previously reported that Raman-SIP is able to link bacterial cells to their ecological functions.^{15,18,21,37} However, this Raman-SIP technology is usually limited by the availability of specific stable isotopically labeled substrates. It is also difficult to apply Raman-SIP to study metabolic activity of cells with complex carbon background in environmental samples. This reverse labeling approach is useful to study the metabolic activity of those substrates when isotopically labeled forms are unavailable or excessively expensive. The application of reverse labeling technology relies on the presence of initially labeled cells, which can be achieved by using readily available ¹³C-compounds such as ¹³C-D-glucose, or via cross-feeding, which

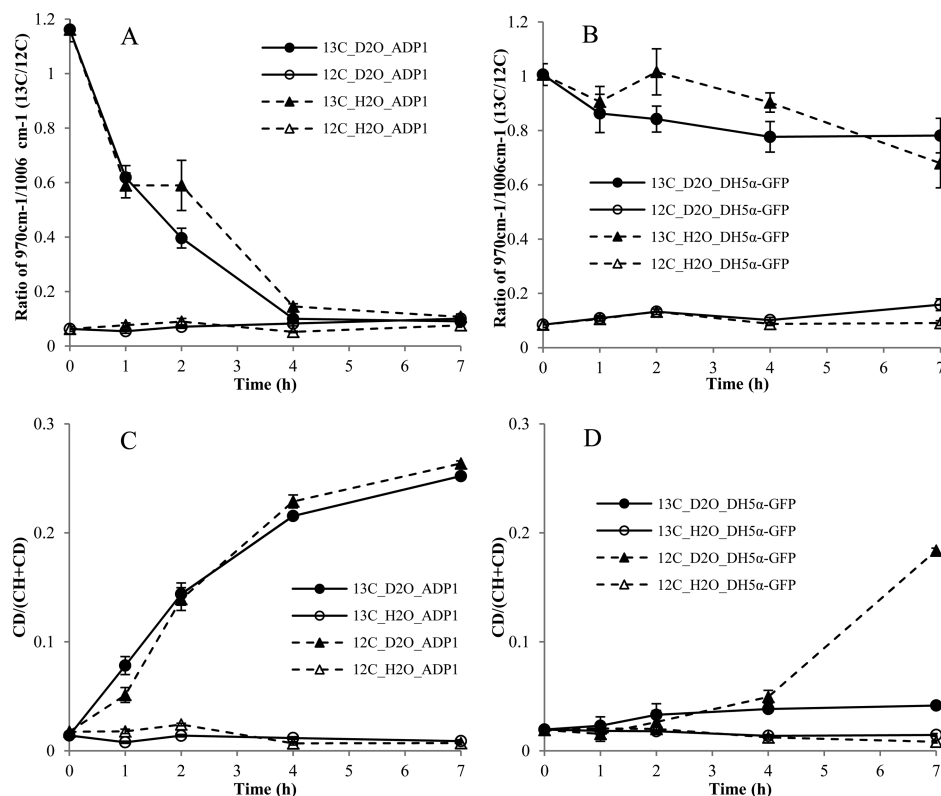


Figure 4. (A) Dynamics of ¹³C replacement by ¹²C incorporation of ADP1 cells in the co-culture of *A. baylyi* ADP1–*E. coli* DH5α-GFP. (B) Dynamics of ¹³C replacement by ¹²C incorporation of DH5α-GFP cells in the co-culture of *A. baylyi* ADP1–*E. coli* DH5α-GFP. (C) Dynamics of deuterium incorporation of ADP1 cells in the co-culture of *A. baylyi* ADP1–*E. coli* DH5α-GFP. (D) Dynamics of deuterium incorporation of DH5α-GFP cells in the co-culture of *A. baylyi* ADP1–*E. coli* DH5α-GFP. Points are the means of spectra from 30 individual cells with 3 biological replicates and error bars show standard deviations.

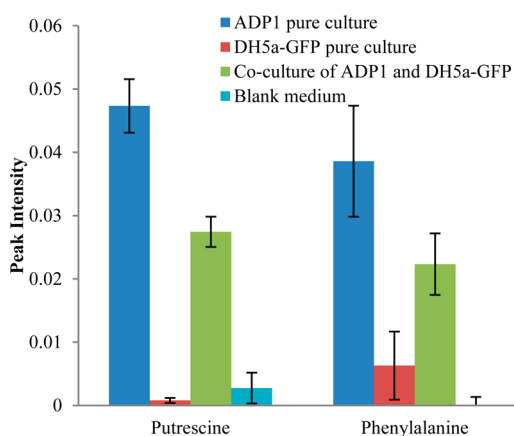


Figure 5. GC/MS analysis results of the metabolites in different cultures. Putrescine and phenylalanine generated by *A. baylyi* ADP1 are responsible for the metabolic activity of *E. coli* DH5α-GFP in the medium with citrate as a sole carbon source. Bars are the means from 5 replicates and error bars show standard deviations.

appears much more common in the natural environment, where communities of bacteria come together to share resources. Here, we have attempted to prove the above concept using a co-culture of ADP1 and DH5α-GFP to metabolize citrate, as the ¹³C-labeled form of citric acid is not available.

Heavy Water (D₂O) Incorporation Is a Universally Sensitive Approach to Indicate General Metabolic Activity in Single Cells. It is well-known that *E. coli* is

unable to use citrate as an energy source under aerobic conditions due to lacking of essential functional genes.^{32,33} The cultivation results of our study confirm that *E. coli* DH5α-GFP was indeed unable to metabolize citrate aerobically, while *A. baylyi* ADP1 was able to use citrate for growth (Figure S4). When citrate was employed as the sole carbon source and D₂O was added in the culture medium, the C–D peak (2040–2300 cm⁻¹) appeared in the SCRS of ADP1 (Figure 1A), indicating high metabolic activity of ADP1 cells. On the contrary, no C–D peak arose for DH5α-GFP at all, even after 7 h of incubation, confirming its inability to assimilate citrate (Figure 1B). However, when ADP1 and DH5α-GFP were cocultivated in MMC, the C–D peak not only appeared in the SCRS of ADP1 (Figure 2C,D) but was also detected in the SCRS of DH5α-GFP as soon as 2 h (Figure 3C,D), although no growth of DH5α-GFP was observed during the 7 h of incubation (Figure S6). The presence of the C–D band reveals incorporation of deuterium from D₂O via NADPH/NADH activity, which associates with general metabolic activity of cells. The C–D peak (2040–2300 cm⁻¹) is located at the “silent zone” (1800–2800 cm⁻¹) which are flat and contain no Raman bands to usual SCRS. Hence, the C–D band appeared at the “silent zone” can be easily distinguished. The above results suggest that Raman-SIP with D₂O labeling could be sensitive and reliable, as it only labeled the live cells that were metabolically active, while inactive cells were unable to incorporate deuterium. Although the high percentage of heavy water could be toxic to plants, animals, and humans, heavy water less than 50% has no significant impact on the growth rate of many microbial strains²¹ including *E. coli* and *A. baylyi* in this case

(Figure S7). Thus, toxicity is not a limiting factor for application of heavy water in Raman-SIP.

Multiple Stable Isotope Probing Is Able to Study Single Cell Metabolism and Interactions in a Microbial Community. A number of characteristic bands in SCRS of ^{13}C -labeled cells such as the benzene ring vibrational band were suggested as suitable biomarkers to quantitatively indicate the ^{13}C content in single cells.²⁰ After 7 h of incubation of the ADP1 and DH5 α -GFP co-culture, SCRS of ^{13}C -ADP1 show that characteristic ^{13}C -band at 970 cm^{-1} reversely shifted back to its corresponding ^{12}C -position at 1006 cm^{-1} (Figure 3A), indicating reverse replacement of ^{13}C by ^{12}C in cells. However, SCRS of ^{13}C -DH5 α -GFP show insignificant change (Figure 3B). This is consistent with the cell counting results in the co-culture, which shows that ADP1 significantly grew but the cell number of DH5 α -GFP remained unchanged after 7 h (Figure S6). Interestingly, the CD band in SCRS of DH5 α -GFP was detectable after 2 h (Figure 3D). Raman-SIP with ^{13}C reverse and D_2O double labeling provide two separate insights of carbon anabolism and general metabolic activity simultaneously at the single cell level. This novel approach is able to differentiate the species responsible for carbon anabolism from those for metabolic activity only. D_2O labeling is also sensitive enough to quantitatively distinct strong, weak active, and inactive cells. Potentially, reverse labeling of ^{15}N -substrate could also be combined with D_2O probing to indicate the nitrogen anabolism as well.

Whilst some reports have claimed that *A. baylyi* would kill active *E. coli* via bacterial type VI secretion system (T6SS), suggesting a hostile predation between *A. baylyi* and *E. coli*,^{38,39} others have reported that *E. coli* can connect to *A. baylyi* via membrane derived nanotubes and exchange nutrients.⁴⁰ These reports suggest that entangled metabolic interactions could occur between *A. baylyi* and *E. coli*. Our findings demonstrated that *E. coli* alone in MMC had no metabolic activity, but became active in the presence of *A. baylyi* (Figure 1B and Figure 3C,D), indicating that *E. coli* can be activated by taking metabolites excreted from *A. baylyi* ADP1. Our complementary analyses using MS-based metabolite footprint analysis suggest that putrescine and phenylalanine could be the candidate metabolites that support metabolic activity of *E. coli*. It suggests that a metabolic interaction-commensalism could happen between *A. baylyi* and *E. coli* mediated by carbon and energy flowing via a food-chain.

The reverse and multiple stable isotope probing can be used as a culture-independent and semiquantitative approach indicating cell metabolism and interactions at the single cell level. This could be applied to study whether cell general metabolic activity is linked to usage of the ^{13}C -labeled substrate. It might be difficult to apply it to a complex environmental sample when multiple carbon sources are available. In these situations, application of reverse and multiple labeling will become complicated as the cells would incorporate ^{12}C from other carbon sources and deuterium from D_2O . However, such difficulty can be overcome by setting a time-course and comprehensive controls. For example, cells that are able to metabolize a specific carbon source could be sorted out by identification of cells with intermediate state of labeling (e.g., 50% ^{12}C and 50% ^{13}C) and comparing cells with controls.

CONCLUSIONS

We have demonstrated a novel Raman-SIP approach coupled with ^{13}C -reverse and D_2O colabeling to study carbon substrate metabolism and microbial interactions in a two-species community. Raman-SIP with reverse labeling would be a useful tool to probe metabolism of any carbon substrates, overcoming limitations when stable isotopic substrates are unavailable. This opens a new door for SIP experiments that cannot be done previously. Raman-SIP with D_2O labeling is growth-independent and universal applicable approach, sensitive enough to probe metabolically active cells without the need of cell replication. This will be particularly valuable to study cell metabolism when the nutrients are not rich enough to support cell multiplication or to probe substrate turnover associated with cellular enzyme activity. This Raman-SIP approach represents an important approach for probing cellular substrate metabolism, metabolic activity, and interactions simultaneously at the single cell level within microbial communities.

ASSOCIATED CONTENT

Supporting Information

The Supporting Information is available free of charge on the ACS Publications website at DOI: 10.1021/acs.analchem.6b01602.

List of the metabolites detected and identified by footprint GC/MS analysis, illustration of the reverse and multiple stable isotope labeling processes, SCRS spectra, main features of Raman spectra, growth curves, combined image of the co-culture of DH5 α -GFP and ADP1 cells, cell counting results, and growth curves (PDF)

AUTHOR INFORMATION

Corresponding Authors

*E-mail: wei.huang@eng.ox.ac.uk. Phone: +44 (0)1865 283786. Fax: +44 (0)1865 374992.

*E-mail: xujian@qibebt.ac.cn.

Notes

The authors declare no competing financial interest.

ACKNOWLEDGMENTS

W.E.H. acknowledges support from EPSRC (Grant EP/M002403/1) and NERC (Grant NE/M002934/1) in the U.K. Y.W. and J.X. acknowledge support from NSFC (Grant 31400436), CAS (Grant XDB15040100), and Shandong Key Project (Grant 2015ZDJS04002) in China. H.M. and R.G. thank the European Commission's Seventh Framework Program for funding (STREPSYNTH; Project No. 613877), and R.G. is also very grateful to BBSRC for financial support and, in particular, for Raman microscopy (Grant BB/L014823/1).

REFERENCES

- (1) Falkowski, P. G.; Fenchel, T.; DeLong, E. F. *Science* **2008**, 320, 1034–1039.
- (2) Little, A. E. F.; Robinson, C. J.; Peterson, S. B.; Raffa, K. E.; Handelsman, J. *Annu. Rev. Microbiol.* **2008**, 62, 375–401.
- (3) Grosskopf, T.; Soyer, O. S. *Curr. Opin. Microbiol.* **2014**, 18, 72–77.
- (4) Handelsman, J. *Microbiol. Mol. Biol. Rev.* **2004**, 68, 669–685.
- (5) Tringe, S. G.; von Mering, C.; Kobayashi, A.; Salamov, A. A.; Chen, K.; Chang, H. W.; Podar, M.; Short, J. M.; Mathur, E. J.; Detter,

- J. C.; Bork, P.; Hugenholtz, P.; Rubin, E. M. *Science* **2005**, *308*, 554–557.
- (6) Amann, R. I.; Ludwig, W.; Schleifer, K. H. *Microbiol. Rev.* **1995**, *59*, 143–169.
- (7) Wang, Y.; Chen, Y.; Zhou, Q.; Huang, S.; Ning, K.; Xu, J.; Kalin, R. M.; Rolfe, S.; Huang, W. E. *PLoS One* **2012**, *7*, e47530.
- (8) Marx, V. *Nat. Methods* **2012**, *9*, 1151–1155.
- (9) Kalisky, T.; Blainey, P.; Quake, S. R. *Annu. Rev. Genet.* **2011**, *45*, 431–445.
- (10) Swan, B. K.; Martinez-Garcia, M.; Preston, C. M.; Sczyrba, A.; Woyke, T.; Lamy, D.; Reinthaler, T.; Poulton, N. J.; Masland, E. D. P.; Gomez, M. L.; Sieracki, M. E.; DeLong, E. F.; Herndl, G. J.; Stepanauskas, R. *Science* **2011**, *333*, 1296–1300.
- (11) Garcia, S. L.; McMahon, K. D.; Martinez-Garcia, M.; Srivastava, A.; Sczyrba, A.; Stepanauskas, R.; Grossart, H.-P.; Woyke, T.; Warnecke, F. *ISME J.* **2013**, *7*, 137–147.
- (12) Kvist, T.; Ahring, B.; Lasken, R.; Westermann, P. *Appl. Microbiol. Biotechnol.* **2007**, *74*, 926–935.
- (13) Marcy, Y.; Ouverney, C.; Bik, E. M.; Loesekann, T.; Ivanova, N.; Martin, H. G.; Szeto, E.; Platt, D.; Hugenholtz, P.; Relman, D. A.; Quake, S. R. *Proc. Natl. Acad. Sci. U. S. A.* **2007**, *104*, 11889–11894.
- (14) Li, M.; Xu, J.; Romero-Gonzalez, M.; Banwart, S. A.; Huang, W. E. *Curr. Opin. Biotechnol.* **2012**, *23*, 56–63.
- (15) Huang, W. E.; Ferguson, A.; Singer, A. C.; Lawson, K.; Thompson, I. P.; Kalin, R. M.; Larkin, M. J.; Bailey, M. J.; Whiteley, A. S. *Appl. Environ. Microb.* **2009**, *75*, 234–241.
- (16) Huang, W. E.; Griffiths, R. I.; Thompson, I. P.; Bailey, M. J.; Whiteley, A. S. *Anal. Chem.* **2004**, *76*, 4452–4458.
- (17) Huang, W. E.; Stoecker, K.; Griffiths, R.; Newbold, L.; Daims, H.; Whiteley, A. S.; Wagner, M. *Environ. Microbiol.* **2007**, *9*, 1878–1889.
- (18) Li, M.; Canniffe, D. P.; Jackson, P. J.; Davison, P. A.; FitzGerald, S.; Dickman, M. J.; Burgess, J. G.; Hunter, C. N.; Huang, W. E. *ISME J.* **2012**, *6*, 875–885.
- (19) Kubryk, P.; Koelschbach, J. S.; Marozava, S.; Lueders, T.; Meckenstock, R. U.; Niessner, R.; Ivleva, N. P. *Anal. Chem.* **2015**, *87*, 6622–6630.
- (20) Li, M.; Huang, W. E.; Gibson, C. M.; Fowler, P. W.; Jousset, A. *Anal. Chem.* **2013**, *85*, 1642–1649.
- (21) Berry, D.; Mader, E.; Lee, T. K.; Woebken, D.; Wang, Y.; Zhu, D.; Palatinszky, M.; Schintmeister, A.; Schmid, M. C.; Hanson, B. T.; Shterzer, N.; Mizrahi, I.; Rauch, I.; Decker, T.; Bocklitz, T.; Popp, J.; Gibson, C. M.; Fowler, P. W.; Huang, W. E.; Wagner, M. *Proc. Natl. Acad. Sci. U. S. A.* **2015**, *112*, E194–E203.
- (22) Uchiyama, T.; Abe, T.; Ikemura, T.; Watanabe, K. *Nat. Biotechnol.* **2005**, *23*, 88–93.
- (23) Huang, W. E.; Wang, H.; Zheng, H. J.; Huang, L. F.; Singer, A. C.; Thompson, I.; Whiteley, A. S. *Environ. Microbiol.* **2005**, *7*, 1339–1348.
- (24) Beceiro, A.; Perez-Llarena, F. J.; Perez, A.; del Mar Tomas, M.; Fernandez, A.; Mallo, S.; Villanueva, R.; Bou, G. *J. Antimicrob. Chemother.* **2007**, *59*, 996–1000.
- (25) Wang, Y.; Ji, Y.; Wharfe, E. S.; Meadows, R. S.; March, P.; Goodacre, R.; Xu, J.; Huang, W. E. *Anal. Chem.* **2013**, *85*, 10697–10701.
- (26) O Faolain, E.; Hunter, M. B.; Byrne, J. M.; Kelehan, P.; McNamara, M.; Byrne, H. J.; Lyng, F. M. *Vib. Spectrosc.* **2005**, *38*, 121–127.
- (27) Fiehn, O.; Wohlgemuth, G.; Scholz, M.; Kind, T.; Lee, D. Y.; Lu, Y.; Moon, S.; Nikolau, B. *Plant J.* **2008**, *53*, 691–704.
- (28) Wedge, D. C.; Allwood, J. W.; Dunn, W.; Vaughan, A. A.; Simpson, K.; Brown, M.; Priest, L.; Blackhall, F. H.; Whetton, A. D.; Dive, C.; Goodacre, R. *Anal. Chem.* **2011**, *83*, 6689–6697.
- (29) Begley, P.; Francis-McIntyre, S.; Dunn, W. B.; Broadhurst, D. I.; Halsall, A.; Tseng, A.; Knowles, J.; Goodacre, R.; Kell, D. B.; Consortium, H. *Anal. Chem.* **2009**, *81*, 7038–7046.
- (30) Dunn, W. B.; Broadhurst, D.; Begley, P.; Zelena, E.; Francis-McIntyre, S.; Anderson, N.; Brown, M.; Knowles, J. D.; Halsall, A.; Haselden, J. N.; Nicholls, A. W.; Wilson, I. D.; Kell, D. B.; Goodacre, R.; Human Serum Metabolome, H. C. *Nat. Protoc.* **2011**, *6*, 1060–1083.
- (31) Sumner, L. W.; Amberg, A.; Barrett, D.; Beale, M. H.; Beger, R.; Daykin, C. A.; Fan, T. W. M.; Fiehn, O.; Goodacre, R.; Griffin, J. L.; Hankemeier, T.; Hardy, N.; Harnly, J.; Higashi, R.; Kopka, J.; Lane, A. N.; Lindon, J. C.; Marriott, P.; Nicholls, A. W.; Reilly, M. D.; Thaden, J. J.; Viant, M. R. *Metabolomics* **2007**, *3*, 211–221.
- (32) Blount, Z. D.; Barrick, J. E.; Davidson, C. J.; Lenski, R. E. *Nature* **2012**, *489*, 513–518.
- (33) Lutgens, M.; Gottschalk, G. *Microbiology* **1980**, *119*, 63–70.
- (34) Prieto-Santos, M. I.; Martin-Checa, J.; Balana-Fouce, R.; Garrido-Pertierra, A. *Biochim. Biophys. Acta, Gen. Subj.* **1986**, *880*, 242–244.
- (35) Kurihara, S.; Tsuboi, Y.; Oda, S.; Kim, H. G.; Kumagai, H.; Suzuki, H. *J. Bacteriol.* **2009**, *191*, 2776–2782.
- (36) Teufel, R.; Mascaraque, V.; Ismail, W.; Voss, M.; Perera, J.; Eisenreich, W.; Haehnel, W.; Fuchs, G. *Proc. Natl. Acad. Sci. U. S. A.* **2010**, *107*, 14390–14395.
- (37) Zhang, D.; Berry, J. P.; Zhu, D.; Wang, Y.; Chen, Y.; Jiang, B.; Huang, S.; Langford, H.; Li, G.; Davison, P. A.; Xu, J.; Aries, E.; Huang, W. E. *ISME J.* **2015**, *9*, 603–614.
- (38) Basler, M.; Ho, B. T.; Mekalanos, J. J. *Cell* **2013**, *152*, 884–894.
- (39) Shneider, M. M.; Buth, S. A.; Ho, B. T.; Basler, M.; Mekalanos, J. J.; Leiman, P. G. *Nature* **2013**, *500*, 350–353.
- (40) Pande, S.; Shitut, S.; Freund, L.; Westermann, M.; Bertels, F.; Colesie, C.; Bischofs, I. B.; Kost, C. *Nat. Commun.* **2015**, *6*, 6238.